

# Scattering of Acoustic and Electromagnetic Waves by an Airfoil

R. T. Ling\* and T. D. Smith†

*Northrop Aircraft Division, Hawthorne, California*

The finite-difference approach based on the generalized scattering amplitude concept is applied to the scattering of acoustic and electromagnetic waves by a two-dimensional airfoil. The transformed Helmholtz equation and associated boundary conditions, in terms of the generalized scattering amplitude, are solved in a numerically generated, body-fitted, curvilinear coordinate system. These are obtained by grid generation procedures commonly used for airfoil aerodynamic computations. Numerical results are obtained for normal incidence of acoustic and electromagnetic waves on a modified NACA 4418 airfoil with a chord length approximately equal to the wavelength of incident waves. The directivity of the scattered sound pressure intensity in the far field is presented in the form of bistatic scattering cross sections. Induced surface current of electromagnetic scattering is also presented. The results of the finite-difference method are in good agreement with those obtained by the method of moments.

## I. Introduction

IN recent years, numerical computations of scattering and diffraction of sound waves by two-dimensional cylindrical bodies and spheres have been attempted by several investigators.<sup>1-5</sup> The scattering phenomena of acoustic and electromagnetic waves are governed by the wave equation, arising from fluid conservation equations in acoustic scattering and from Maxwell's equations in electromagnetic scattering. A major difficulty in solving the scattering problem lies in the enforcement of surface boundary conditions for an arbitrarily shaped obstacle. This difficulty limits the applicability of the eigenfunction expansion method<sup>6-8</sup> to simple obstacle shapes such as infinite circular cylinders and spheres. Several numerical schemes<sup>9,10</sup> have been devised to generate body-fitted, curvilinear coordinate systems to alleviate a similar difficulty in computational fluid dynamics (CFD) problems involving complex aircraft configurations.

An application of grid generation techniques to scatterings of acoustic and electromagnetic waves by arbitrarily shaped, two-dimensional cylinders is presented in this paper, using an airfoil as an example. The capability to align grid points on the obstacle surface offers great advantages over fixed Cartesian grids, in either differential or integral equation approaches to the scattering problem. One type of differential equation formulation that allows the application of grid generation techniques to numerical treatment of scattering problems is based on the generalized scattering amplitude concept.<sup>1,5,11</sup> This theory has been applied successfully to wave scatterings by infinite circular cylinders and spheres.<sup>1,5,11,12</sup> The cylindrical and spherical coordinates used in these example problems are the natural body-fitted, curvilinear coordinate systems. When the theory is applied to complex geometry obstacles, numerical results are obtained by solving the governing equation and associated boundary conditions in the numerically generated boundary-fitted, curvilinear coordinate systems. The basis of this approach is the similarity between fluid dynamics and electromagnetics problems as boundary value problems involving identical obstacle geometry.<sup>11</sup>

## II. Differential Equation Formulation for the Generalized Scattering Amplitude in Body-Fitted Coordinates

For the sake of simplicity, the discussion in this section will be limited to acoustic wave scattering. The correspondence between two-dimensional acoustic scattering and the equivalent problem of a two-dimensional electromagnetic scattering will be made in Sec. IV. The problem under consideration is the scattering of a plane wave, incident normally upon an infinitely long, airfoil-shaped cylinder, at rest in the fluid medium in which the sound waves propagate. The schematics of the scattering problem and coordinate systems are illustrated in Figs. 1 and 2.

The incident sound wave of wavelength  $\lambda$  and frequency  $\nu$  propagates in the direction of wave number vector  $\mathbf{k}$  that lies on the  $x$ - $y$  plane and makes an angle  $\Theta$  with the  $x$  axis. The incident plane wave is represented by  $\exp[i(\mathbf{k} \cdot \mathbf{r} - \omega t)]$ , where  $\mathbf{r}$  is the radius vector on the  $x$ - $y$  plane,  $|\mathbf{k}| = 2\pi/\lambda$  the wave number, and  $\omega = 2\pi\nu$  the angular frequency. The axis of the airfoil cylinder lies along the  $z$  axis. For an inviscid fluid at rest, the sound pressure and the velocity potential satisfy the wave equation, which reduces to the Helmholtz equation by assuming a time-harmonic dependence  $\exp\{-i\omega t\}$  for all dependent variables.

Based on the generalized scattering amplitude concept, the total wave  $\phi$ , representing either the sound pressure or the velocity potential throughout the scattering region, can be written as a superposition of the incident plane wave and the scattered wave as

$$\phi = e^{ikx} + f(r, \theta)e^{ikr/\sqrt{kr}} \quad (1)$$

The scattered wave contains the generalized scattering amplitude  $f(r, \theta)$ , modulated by an outgoing cylindrical wave. The transformed Helmholtz equation, in terms of the generalized scattering amplitude, is given by<sup>1</sup>

$$\frac{\partial^2 f}{\partial r^2} + 2ik \frac{\partial f}{\partial r} + \frac{1}{r^2} \frac{\partial^2 f}{\partial \theta^2} + \frac{1}{4r^2} f = 0 \quad (2)$$

in the cylindrical coordinate system.

In the finite-difference approach to solving differential equations and enforcing boundary conditions for a physical system, it is desirable to have a constant coordinate surface

Received Nov. 16, 1987; presented as Paper 88-0180 at the AIAA 26th Aerospace Sciences Meeting, Reno, NV, Jan. 11-14, 1988; revision received May 25, 1988. Copyright © American Institute of Aeronautics and Astronautics, Inc., 1988. All rights reserved.

\*Senior Technical Specialist. Member AIAA.

†Senior Engineer. Member AIAA.

coinciding with the physical boundary. This ensures that a set of grid points falls right on the body surface, eliminating the need for interpolation of physical variables in satisfying the body surface boundary condition. Computer codes<sup>9,10</sup> that automatically generate the body-fitted coordinate systems have become commonplace in the last decade, particularly among aerodynamicists dealing with complex aircraft geometry. These grid generation codes, which produce grids for the aerodynamic computation of an airfoil, also can provide grids for the computation of acoustic and electromagnetic wave scatterings by an airfoil.

Since most grid generation codes use Cartesian coordinates for the description of body-fitted grid points in the preliminary step of physical space definition, the transformed Helmholtz equation in cylindrical coordinates, as shown in Eq. (2), is first transformed into Cartesian coordinates and becomes

$$\frac{\partial^2 f}{\partial x^2} + \frac{\partial^2 f}{\partial y^2} + \left( 2ik \frac{x}{\sqrt{x^2 + y^2}} - \frac{x}{x^2 + y^2} \right) \frac{\partial f}{\partial x} + \left( 2ik \frac{y}{\sqrt{x^2 + y^2}} - \frac{y}{x^2 + y^2} \right) \frac{\partial f}{\partial y} + \frac{1}{4} \frac{1}{x^2 + y^2} f = 0 \quad (3)$$

Equation (3) then is transformed into the computational space body-fitted coordinate system  $(\xi, \eta)$  and becomes

$$A \frac{\partial^2 f}{\partial \xi^2} + B \frac{\partial^2 f}{\partial \xi \partial \eta} + C \frac{\partial^2 f}{\partial \eta^2} + D \frac{\partial f}{\partial \xi} + E \frac{\partial f}{\partial \eta} + Gf = 0 \quad (4)$$

where coefficients  $A, B, C$ , etc., involve components of the covariant metric tensor of the body-fitted coordinate system. The coefficient of the cross-derivative term  $B$  vanishes where the body-fitted grids are orthogonal.

The acoustic pressure vanishes on the surface of an acoustically soft airfoil and the normal component of the fluid velocity vector vanishes on the surface of an acoustically hard airfoil. Therefore, in the body-fitted coordinate system, the surface boundary condition for the total wave assumes a simple Dirichlet condition

$$\phi(\xi, \eta_0) = 0 \quad (5a)$$

for an acoustically soft airfoil and a simple Neumann condition

$$\left( \frac{\partial \phi}{\partial \hat{n}(\eta)} \right)_{\eta = \eta_0} = 0 \quad (5b)$$

for an acoustically hard airfoil. In Eqs. (5a) and (5b),  $\eta = \eta_0$  is the computational space constant coordinate line that coincides with the airfoil surface profile in the physical space, while  $\hat{n}(\eta)$  is the unit normal vector pointing outward from the airfoil surface. If the body-fitted grids are orthogonal on the obstacle surface, the surface boundary condition [Eq. (5b)] reduces to

$$\left( \frac{\partial \phi}{\partial \eta} \right)_{\eta = \eta_0} = 0 \quad (5c)$$

for an acoustically hard airfoil.

The corresponding boundary conditions for the generalized scattering amplitude in the body-fitted coordinates can be readily derived using Eq. (1). The surface boundary condition corresponding to Eq. (5a) retains the Dirichlet form for an acoustically soft airfoil

$$f(\xi, \eta_0) = g(\xi) \quad (6a)$$

where  $g(\xi)$  is a known function of  $\xi$ . Equation (5c) assumes the form

$$\alpha(\xi)f(\xi, \eta_0) + \beta(\xi) \left( \frac{\partial f}{\partial \eta} \right)_{\eta = \eta_0} + \gamma(\xi) = 0 \quad (6b)$$

where  $\alpha, \beta$ , and  $\gamma$  are known functions of  $\xi$ . If the body-fitted grids are nonorthogonal on the obstacle surface, the boundary condition corresponding to Eq. (5b) would contain additional terms involving derivatives with respect to  $\xi$ . Thus, it would become somewhat more complicated than Eq. (6b). The radiation condition retains the simple Neumann type

$$\lim_{\eta \rightarrow \infty} \frac{\partial f(\xi, \eta)}{\partial \eta} = 0 \quad (7)$$

if constant  $\eta$  lines become large circles in the far field.

Equations (4), (6), and (7) mathematically define the boundary value problem of sound wave scattering by an arbitrarily shaped two-dimensional airfoil. The solution of the generalized scattering amplitude over the computational space of  $\xi$  and  $\eta$  completely determines the scattered waves in the physical space. The primary concern of an investigation into a scattering problem is often the determination of the far-field scattering amplitudes. The scattering amplitudes in acoustic scatterings provide the information on the directivity of the far-field scattered sound pressure intensity. In the present formulation, this information is given by the bistatic acoustic cross sections defined in Ref. 1.

### III. Numerical Results and Discussions

This theory has been applied to the scattering of sound waves by an airfoil, with solutions obtained by the finite-difference method described in Ref. 1. The circular cylinder problem solved in Ref. 1 involves the simplest two-dimensional shape. The cylindrical coordinates used are the natural body-fitted grids. To ensure accurate and correct working of the grid generation and solver codes developed to solve Eqs. (4), (6), and (7) for the airfoil scattering problem, these codes first were applied to the circular cylinder scattering. The numerical results reported in Ref. 1 for both soft and hard cylinders were reproduced.

The geometry and body-fitted grids for the airfoil considered in this paper are shown in Figs. 3–5. The airfoil profile as shown in Fig. 3 is a modified NACA 4418 airfoil with the

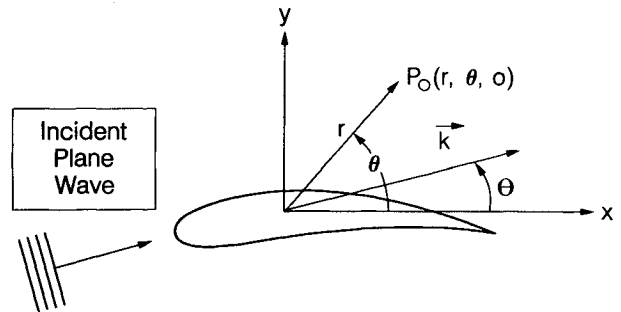


Fig. 1 Normal incidence of a plane wave on an airfoil.

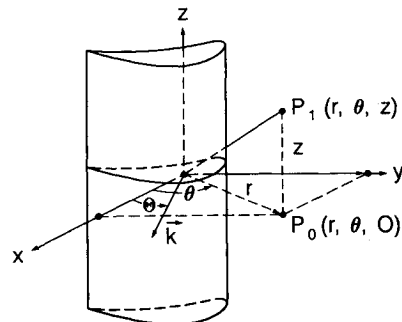


Fig. 2 Airfoil cylinder geometry.

original trailing edge (last 5% of the chord length) rounded off. The reason for the modification is to avoid, for the time being, the uniqueness problem<sup>8,15</sup> in numerical solutions related to a sharp edge. Let  $\ell$  denote the chord length of the airfoil. The incident wavelength is chosen so that the dimensionless electrical length  $k\ell$  of the airfoil is equal to 5.952. As a consequence, the wavelength is equal to  $1.0556\ell$ , slightly longer than the chord length. The O-type grids shown in Figs. 4 and 5 are generated by an algebraic grid generation method,<sup>13</sup> which also provides the metric tensor for the computation of the coefficients in Eq. (4). For convenience, the chordwise direction is assumed to lie along the  $x$  axis. Grid points are densely packed near the airfoil surface where large gradients in the generalized scattering amplitudes are expected. Since the generalized scattering amplitudes asymptotically approach their limiting values in the far field, much coarser grids are used away from the airfoil. The outermost constant  $\eta$  line generated corresponds to a large circle with a radius roughly equal to 50 chord lengths. For incident wavelengths approximately equal to the chord length, a network of  $40(\xi) \times 52(\eta)$  grid points is sufficient to resolve the angular variation in bistatic cross sections. Typical CPU time for grid generation and computation of bistatic cross sections for such a network is less than 2 min on an IBM 3081 computer. In order to obtain somewhat smoother curves, the results presented in this paper are computed with finer grids,  $72 \times 72$  for the soft airfoil and  $96 \times 72$  for the hard airfoil.

#### Acoustically Soft Airfoil

The dependence of bistatic acoustic cross sections on polar angle  $\theta$  for an acoustically soft airfoil with its profile given by Fig. 3 is shown in Figs. 6 and 7 for incident angles  $\Theta$  at 0 and  $\pi$ , respectively. The bistatic cross sections are plotted in decibel scales for the dimensionless ratio of the two-dimensional bistatic cross section over the wavelength. The agreement between the prediction of the present method and that of the moment method<sup>14</sup> (a 90-element solution) is excellent for all scattering and incident angles.

The moment method refers to a broad class of basis function projection methods applied to the integral equation representation of the electromagnetic fields in terms of sources within and fields on the obstacle surface. The particular method of moments used for comparison purpose in this paper employs pulse basis functions, which provide uniform current over each surface element.

Generally, the basis functions used in a moment method are nonorthogonal. The resultant moment matrix, which accounts for the interactions between pairs of surface or volume elements, has nonzero elements everywhere. As a consequence, the computer memory requirement for a moment method is at least  $N^2$ , where  $N$  is the number of unknowns. In contrast to this, the associated matrix resulted from the present finite-difference approximation to the transformed Helmholtz equation is a sparse matrix with nonzero elements along a small number (approximately 10) of diagonals to account for the interactions

between unknowns at a grid point to those at the neighboring grid points. The computer memory requirement for the finite-difference method is on the order of  $10N$ .

For a perfectly hard or soft cylinder, the surface integral equation formulation of the moment method reduces the problem to an equivalent one-dimensional problem, involving only the unknowns on the cylinder's surface. In this special case, the moment method is somewhat more efficient than the finite-difference method if the number of unknowns is not too large. For example, a 90-element moment method takes about 15 s CPU time on a VAX 11/780 machine. The corresponding run time on an IBM 3081 machine would be about 2 s CPU

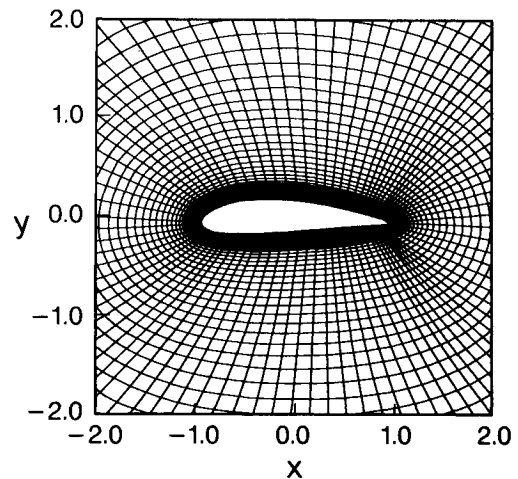


Fig. 4 Near-field grid distribution.

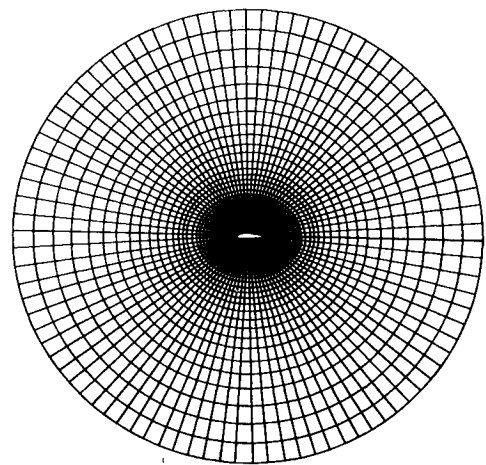


Fig. 5 Global grid distribution.

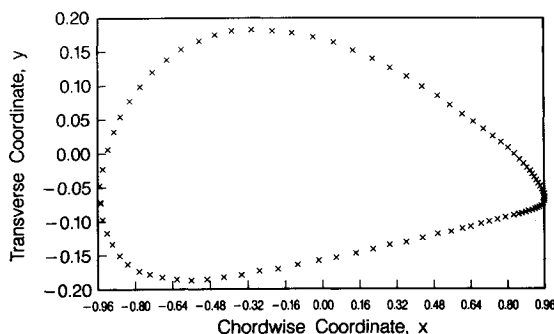


Fig. 3 Profile of the modified NACA 4418 airfoil.

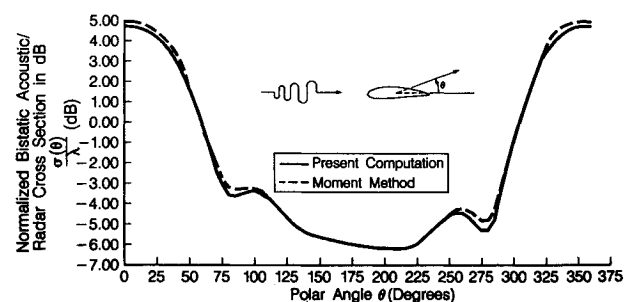


Fig. 6 Bistatic acoustic/radar cross section for the modified NACA 4418 airfoil ( $\lambda = 1.0556\ell$ ,  $\Theta = 0$ , soft airfoil, E polarization).

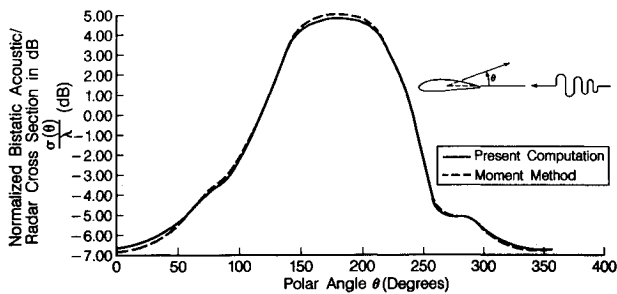


Fig. 7 Bistatic acoustic/radar cross section for the modified NACA 4418 airfoil ( $\lambda = 1.0556\ell$ ,  $\Theta = \pi$ , soft airfoil, E polarization).

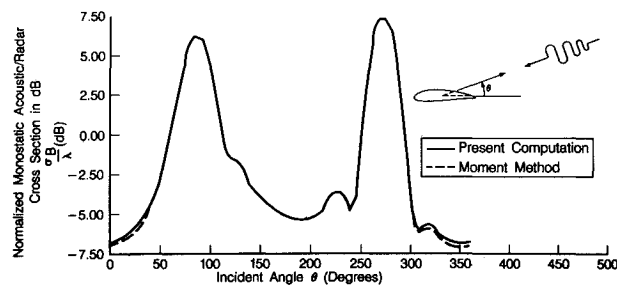


Fig. 8 Monostatic acoustic/radar cross section for the modified NACA 4418 airfoil ( $\lambda = 1.0556\ell$ , soft airfoil, E polarization).

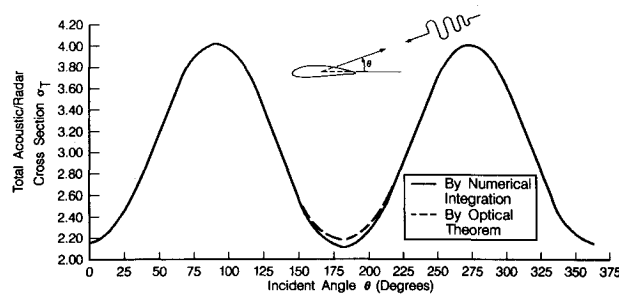


Fig. 9 Total acoustic/radar cross section for the modified NACA 4418 airfoil ( $\lambda = 1.0556\ell$ , soft airfoil, E polarization).

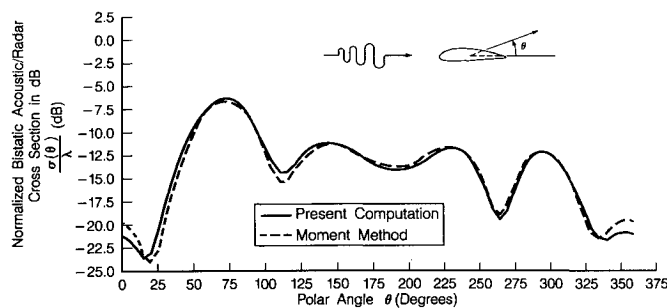


Fig. 10 Bistatic acoustic/radar cross section for the modified NACA 4418 airfoil ( $\lambda = 1.0556\ell$ ,  $\Theta = 0$ , hard airfoil, H polarization).

time, substantially faster than a two-dimensional difference computation. However, due to its full matrix structure, the advantage of moment methods disappears when higher frequencies or shorter wavelengths are approached. In a volumetric integral equation formulation for imperfectly hard and soft cylinders, the number of unknowns is roughly equal in both the moment and finite-difference methods. In these cases, the moment methods are more computationally intensive and require more memory storage.

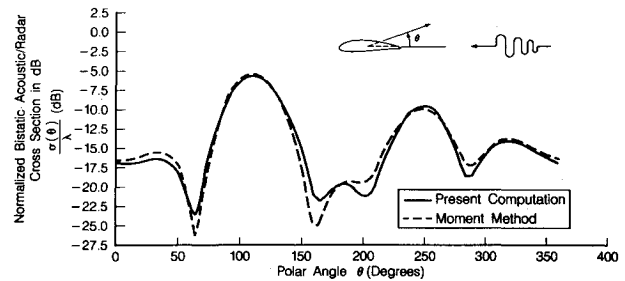


Fig. 11 Bistatic acoustic/radar cross section for the modified NACA 4418 airfoil ( $\lambda = 1.0556\ell$ ,  $\Theta = \pi$ , hard airfoil, H polarization).

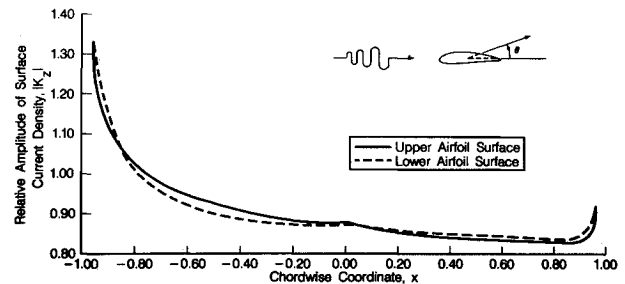


Fig. 12 Distribution of relative amplitude of surface current density ( $\lambda = 1.0556\ell$ ,  $\Theta = 0$ , soft airfoil, E polarization).

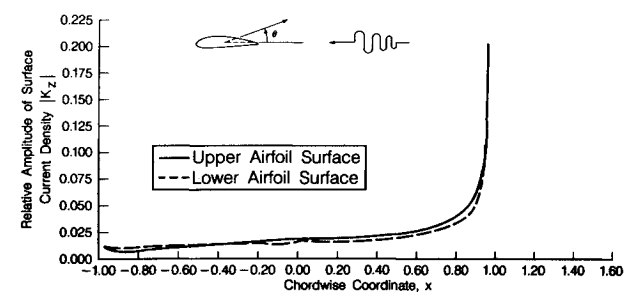


Fig. 13 Distribution of relative amplitude of surface current density ( $\lambda = 1.0556\ell$ ,  $\Theta = \pi$ , soft airfoil, E polarization).

At present, the solutions for the generalized scattering amplitude are obtained by directly inverting the matrix resulting from the finite-difference method of Ref. 1. For scattering by an acoustically soft obstacle, the changes in the Dirichlet-type boundary condition due to different incident angles do not alter the matrix to be inverted. Since the elements of the inverse matrix are stored in the inversion process, little extra CPU time is required to obtain solutions for different incident angles. This property was taken advantage of in obtaining the monostatic sweep of backscattering cross sections, as illustrated in Fig. 8. Except for small differences near incidences toward the trailing edge, results from the present method cannot be distinguished from those of the moment method.

Figure 9 shows the total scattering cross sections as the incident waves sweep around the airfoil. The total cross sections computed from numerical integration of bistatic cross sections are compared with those obtained by applications of the optical theorem. Only a slight deviation occurs near incidences toward the leading edge, where the optical theorem is off by about 2%.

#### Acoustically Hard Airfoil

For scatterings by an acoustically hard airfoil, the bistatic acoustic cross sections are plotted vs polar angles in Figs. 10 and 11 for incident angles  $\Theta$  at 0 and  $\pi$ . Close agreement is

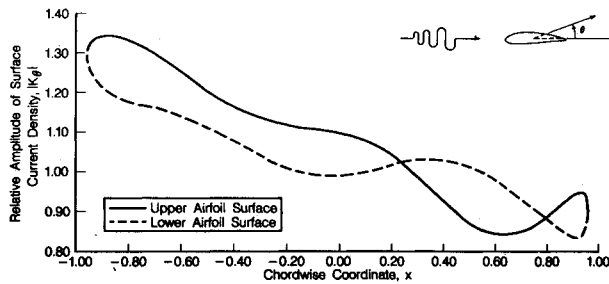


Fig. 14 Distribution of relative amplitude of surface current density ( $\lambda = 1.0556$ ,  $\theta = 0$ , hard airfoil, H polarization).

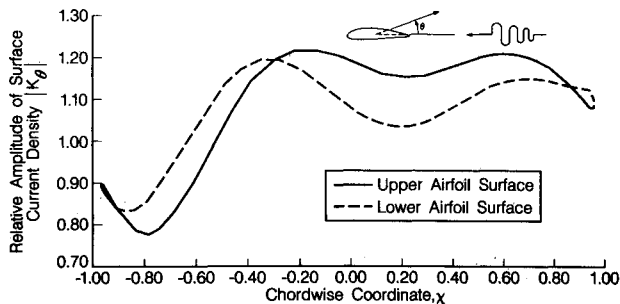


Fig. 15 Distribution of relative amplitude of surface current density ( $\lambda = 1.0556$ ,  $\theta = \pi$ , hard airfoil, H polarization).

obtained between the results from the present method and those from the moment method.

The application of body-fitted, curvilinear coordinate systems demonstrated above for two-dimensional acoustic scatterings can be readily generalized to three-dimensional (3-D) acoustic scattering problems.<sup>5</sup> As in two-dimensional cases, the acoustically soft and hard cases can be treated separately.

#### IV. Equivalent Electromagnetic Scattering

For a plane electromagnetic wave normally incident on an infinitely long, perfectly conducting cylinder, with the incident electric field parallel to the cylindrical axis (the E-polarization case), the axial component of the total electric field satisfies exactly the same governing equation and boundary conditions as the sound pressure in the sound wave scattering by an acoustically soft cylinder. Similarly, the electromagnetic wave scattering, with the incident magnetic field parallel to the cylindrical axis (the H-polarization case), is mathematically equivalent to the sound scattering by an acoustically hard cylinder. Therefore, the bistatic acoustic cross sections given in Sec. III can be interpreted as the bistatic radar cross sections of a perfectly conducting airfoil.

In electromagnetic wave scattering, the electric current induced on the airfoil surface is also of interest. The induced surface current can be regarded as a source from which the scattered fields are generated. In the integral equation methods, such as the method of moments, the surface current density  $\mathbf{K} = \hat{n} \times \mathbf{H}$  is the basic unknown to be solved and from which the scattered fields and bistatic cross sections are to be computed. In the E-polarization case, the induced surface current flows along the cylindrical axis with its complex value given by

$$\left[ \frac{\partial E_z}{\partial \hat{n}(\eta)} \right]_{\eta} = \eta_0$$

In the H-polarization case, the induced surface current flows tangentially on the airfoil surface in a direction perpendicular to the cylindrical axis, with its complex value given by  $H_z(\xi, \eta_0)$ , the value of the magnetic field on the airfoil surface. Chordwise distributions of relative amplitudes of induced surface current densities on the upper and lower airfoil surfaces for  $\theta = 0$  and  $\pi$  in the E-polarization case are shown in Figs. 12 and 13. Corresponding results for the H-polarization case are shown in Figs. 14 and 15.

Electromagnetic wave scattering by arbitrarily shaped three-dimensional obstacles is governed by the vector wave equation or the vector Helmholtz equation for electric and magnetic field vectors. It becomes a scalar problem only in the case of scatterings by two-dimensional cylindrical bodies, under normal incidence and appropriate polarization conditions, as discussed in this paper. However, it is interesting to note that a three-dimensional electromagnetic scattering problem can be reduced to two independent scalar scattering problems, in much the same way that the three-dimensional acoustically soft and hard scatterings are separated. To achieve this reduction, it is necessary to formulate the electromagnetic scattering problem in terms of a pair of scalar Debye potentials.<sup>11,15-17</sup> These satisfy the scalar Helmholtz equation and can be used to generate the electric and magnetic field vectors. For a perfectly conducting sphere, the media interface conditions for the two Debye potentials are identical in form to those for the acoustic pressure (soft sphere case) and the velocity potential (hard sphere case) in the corresponding acoustic scattering.<sup>5,11</sup>

#### V. Conclusions

The results presented here demonstrate that the difficulty associated with the enforcement of surface boundary conditions in wave scattering problems due to complex obstacle geometry can be alleviated by employing the grid generation techniques developed for computational fluid dynamics (CFD). Rapid progress in CFD in recent years has provided many useful tools that can be used for numerical treatment of wave scattering problems. This paper offers an excellent example.

#### Acknowledgments

This work was performed under Northrop's Independent Research and Development Program. The authors wish to express their appreciation to Messrs. M. W. George and H. A. Gerhardt for managerial support of this study. They also thank Dr. B. Horning for providing the method-of-moments results.

#### References

- Ling, R. T. "Numerical Solution for the Scattering of Sound Waves by a Circular Cylinder," *AIAA Journal*, Vol. 25, April 1987, pp. 560-566.
- Khan, M. M. S., Brown, W. H., and Ahuja, K. K., "Computational Aeroacoustics as Applied to the Diffraction of Sound by Cylindrical Bodies," *AIAA Journal*, Vol. 25, July 1987, pp. 949-956.
- SenGupta, G. and Sidwell, K. W., "Computation of Aeroacoustic Scattering Effects," *AIAA Paper 87-2669*, Oct. 1987.
- Khan, M. M. S., "Diffraction of Sound Waves by an Airfoil in Moving Media," *AIAA Paper 87-2670*, Oct. 1987.
- Ling, R. T., "Finite Difference Approach to Scattering of Sound Waves in Fluids," *AIAA Journal*, Vol. 26, Feb. 1988, pp. 151-155.
- Morse, P. M., *Vibration and Sound*, McGraw-Hill, New York, 1948.
- King, R. W. P. and Wu, T. T., *The Scattering and Diffraction of*

*Waves*, Harvard Univ. Press, Cambridge, MA, 1959.

<sup>8</sup>Bowman, J. J., Senior, T. B. A., and Uslenghi, P. L. E., *Electromagnetic and Acoustic Scattering by Simple Shapes*, North-Holland, Amsterdam, 1969.

<sup>9</sup>Thompson, J. F., Warsi, Z. U. A., and Masten, C. W., *Numerical Grid Generation: Foundation and Applications*, North-Holland, Amsterdam, 1985.

<sup>10</sup>Smith, R. E. (Ed.), *Numerical Grid Generation Techniques*, NASA CP-2166, Oct. 1980.

<sup>11</sup>Ling, R. T., "Application of Computational Fluid Dynamics (CFD) Methods to a Numerical Study of Electromagnetic Wave Scattering Phenomena," *Journal of Applied Physics*, Vol. 64, Oct. 1988, pp. 3785-3791.

<sup>12</sup>George, M. W., Ling, R. T., Mangus, J. F., and Thompkins, W.

T., "Application of Computational Physics within Northrop," in "Supercomputing in Aerospace," NASA CP-2454, March 1987, pp. 125-137.

<sup>13</sup>Smith, T. D., "An Algebraic Grid Generation Technique Utilizing Parametric Cubic Equations," Northrop Aircraft, Hawthorne, CA, Rept. 87-58, May 1987.

<sup>14</sup>Harrington, R. F., *Field Computation by Moment Methods*, MacMillan, New York, 1968.

<sup>15</sup>Ivanov, Y. A., "Diffraction of Electromagnetic Waves on Two Bodies," NASA TT F-597, April 1970.

<sup>16</sup>Bromwich, T. J. I'A., "Electromagnetic Waves," *Philosophical Magazine*, Vol. 38, 1919, pp. 143-163.

<sup>17</sup>Born, M. and Wolf, E., *Principles of Optics*, Pergamon, New York, 1980.

*Recommended Reading from the AIAA  
Progress in Astronautics and Aeronautics Series . . .*



## **Dynamics of Flames and Reactive Systems and Dynamics of Shock Waves, Explosions, and Detonations**

*J. R. Bowen, N. Manson, A. K. Oppenheim, and R. I. Soloukhin, editors*

The dynamics of explosions is concerned principally with the interrelationship between the rate processes of energy deposition in a compressible medium and its concurrent nonsteady flow as it occurs typically in explosion phenomena. Dynamics of reactive systems is a broader term referring to the processes of coupling between the dynamics of fluid flow and molecular transformations in reactive media occurring in any combustion system. *Dynamics of Flames and Reactive Systems* covers premixed flames, diffusion flames, turbulent combustion, constant volume combustion, spray combustion nonequilibrium flows, and combustion diagnostics. *Dynamics of Shock Waves, Explosions and Detonations* covers detonations in gaseous mixtures, detonations in two-phase systems, condensed explosives, explosions and interactions.

### **Dynamics of Flames and Reactive Systems**

1985 766 pp. illus., Hardback  
ISBN 0-915928-92-2  
AIAA Members \$54.95  
Nonmembers \$84.95  
Order Number V-95

### **Dynamics of Shock Waves, Explosions and Detonations**

1985 595 pp., illus. Hardback  
ISBN 0-915928-91-4  
AIAA Members \$49.95  
Nonmembers \$79.95  
Order Number V-94

TO ORDER: Write AIAA Order Department, 370 L'Enfant Promenade, S.W., Washington, DC 20024. Please include postage and handling fee of \$4.50 with all orders. California and D.C. residents must add 6% sales tax. All orders under \$50.0 must be prepaid. All foreign orders must be prepaid. Please allow 4-6 weeks for delivery. Prices are subject to change without notice.